NAIC-ID(RS)T-0495-95

NATIONAL AIR INTELLIGENCE CENTER

LASER GUIDE STARS AND NEAR-INFRARED Na_2 OSCILLATION

(Selected Articles)

**Approved for public release:
distribution unlimited**

HUMAN TRANSLATION

NAIC-ID(RS)T-0495-95 6 December 1995

MICROFICHE NR: 95C000756

LASER GUIDE STARS AND NEAR-INFRARED Na_2 OSCILLATION
(Selected Articles)

English pages: 41

Source: Jiguang Jishu, Vol. 17, Nr. 2, April 1993;
pp. 65-74; 78-82; 112-113

Country of origin: China
Translated by: Leo Kanner Associates
F33657-88-D-2188
Requester: NAIC/TATD/Bruce Armstrong
Approved for public release: distribution unlimited.

TABLE OF CONTENTS

GRAPHICS DISCLAIMER

All figures, graphics, tables, equations, etc. merged into this translation were extracted from the best quality copy available.

LASER GUIDE STARS FOR ADAPTIVE OPTICAL SYSTEM WITH PARTIAL CORRECTION

Yan Jixiang, Zhou Renzhong, and Yu Xin
Department of Engineering Optics,
Beijing University of Science and
Engineering, Beijing 10081

Abstract: In this article, the number of the artificial guide stars and the brightness of the guide stars used in the partial-correction adaptive optical system with 0.5 Strehl rate(or 0.13 residual rms wavefront error over the subaperture) have been presented. Comparing to the correspondent results of the conventional system, we find that the partial correction system is simple and easy to realize.

I. Introduction

Random phase fluctuations due to atmospheric eddy currents seriously restrict the resolving power of large ground-based astronomical telescopes. In good visibility, the typical resolving power for visible-light wavelengths is only about 1rad/s. By adopting adaptive optics with wavefront compensation, this situation can be significantly improved, achieving imaging quality near the diffraction limit.

An adaptive optical system is composed of fundamental

components: wavefront sensor and wavefront corrector. The function of the wavefront sensor is to detect anomalous wavefronts at the telescope pupil plane. Normal operating conditions are that there should be a certain photon current inside the subapertures. When the brightness of the object to be imaged is weak, reference stars that are bright enough in the same isoplanatic region are required. However, since the isoplanatic angle in the atmosphere is very small, and since natural guide stars are too few to cover the entire sky, many objects to be observed lack sufficient brightness and there are no guide stars in the vicinity with sufficient brightness. Foy et al. [1] was the earliest to propose, in 1985, that artificial guide stars can be generated by using a laser in the upper atmospheric layers. Since lasers can be directed in any direction, the artificial stars are able to cover the entire sky. Two years later, Thompson [2] developed this concept in two aspects. On the one hand, he calculated the key engineering parameters for generating artificial guide stars. On the other hand, he was successful for the first time in generating artificial guide stars in the sodium layer over the Mauna Kea optical observatory in Hawaii, on the night of January 21 of that year. In recent years, the problem of artificial guide stars became a very active area of research in adaptive optics.

Interest in adaptive optics involves mainly compensating for wavefront anomalies caused by eddy currents in the atmosphere. In seeking perfect correction, the complex structure and high costs compel users to begin considering the possibility of partial

correction. Hardy was the earliest scientist to propose adaptive optics in the 1991 annual conference of the International Society of Photographic Engineering (SPIE). He proposed to treat them separately: the laser emitted adaptive optical system and the astronomical imaging adaptive optical system. Moreover, he pointed out, in applications for the latter case, Strehl ratio is 0.5 or smaller, images with near-diffraction-limit resolution can still be obtained. When compared with the requirements on guide stars, in the traditional system as reported in the literature, we can see that guide stars in a partial-correction system are realized much more easily.

II. Strehl Ratio and Rms Wavefront Error

The Strehl ratio (S) was first introduced by German scientist Strehl while studying point-source imaging in 1902. The Strehl ratio is defined as the ratio between the peak value intensities of anomalous wavefronts and anomaly-free wavefronts. The relationship between $\Delta\phi$ of S with wavelength taken as unity can be approximated by

$$S = \exp\{-(2\pi\Delta\varphi/\lambda)^2\} \qquad (1)$$

When the wavefront anomaly is serious, there is no simple relationship between S and $\Delta\phi$. However, only if $S \geq 0.3$, we can derive [3,4] $[1-(S/S_0 \times 100\% \leq 10\%$. In the equation, S_0 is the precise value of the Strehl ratio. This article discusses the situation when $S \approx 0.5$. Therefore, by using Eq. (1), the percentage error of the theoretical value of S derived is less than 10%. Substitute

percentage error of the theoretical value of S derived is less than 10%. Substitute S=0.5 into Eq. (1) and we get

$$\Delta\varphi \approx 0.13\lambda$$

This is the corresponding rms wavefront difference at the aperture.

III. Number of Artificial Guide Stars Required for Partial Correction System

Assume that the isoplanatic angle in the atmosphere is Θ_{ip}, and that the height of the guide stars over the pupillary plane of the telescope is h_0, then the diameter of a guide star in the region covered by the telescope aperture is defined as (see attached figure)

$$D_{ip} = 2h_0\theta_{ip} \tag{2}$$

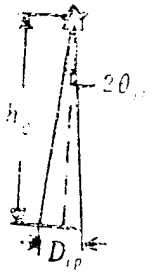

Fig. Area covered with starlight at telescope aperture cross section

Use D_0 to indicate the maximum telescope aperture for which there is only one guide star, and mark D_0 as

$$D_0 = D_{ip}/\alpha = 2h_t\theta_{ip}/\alpha \qquad (3)$$

In the equation, a is determined by the rms residual wavefront difference of the maximum allowable value on the aperture plane, and is related to the atmospheric mode. Here, two modes are considered: one is under the assumption that the eddy currents in the atmosphere appear only in a thin layer with height h_t, and it is briefly referred to as the model of a single thin layer. Another mode is the model assumed by Hufnagel, that is,

$$C_n^2(h) = 2.2\times10^{-23}h^{10}e^{-h} + 10^{-16}e^{-h/1.5}$$

With respect to $\Delta\phi=0.13\lambda$, then a (corresponding to the first model) is about 0.7. Corresponding to the second mode, a is approximately 0.8 [5]. In addition, the atmospheric isoplanatic angle of any eddy current coinciding with the previous model is

$$\theta_{ip} \approx r_0/3h_t$$

However, the atmospheric isoplanatic angle matching the latter model is

$$\theta_{ip} \approx 4\times10^{-5}r_0$$

In the equation, m is the unit for the Freid constant. However, measurements for Θ_{ip} are in radians. It is assumed that the height at which eddy currents appear in the single thin layer model is h_t=10km. Substitute the above-mentioned results into Eq. (3), then we obtain the two models, respectively,

$$D_0 = (20/21)\times10^{-4}h_tr_0$$

and

$$D_0 = 1\times10^{-4}h_tr_0$$

However, the numbers of guide stars required for a telescope with an overall aperture D for

$$N_s = (20D/21h_tr_0)^2\times10^8 \qquad (4)$$

and

$$N_s = (D/h_s r_0)^2 \times 10^3 \qquad (5)$$

When we compare Eqs. (4) and (5), we can see that for both the atmospheric models (but assuming equal r_0), the numbers of guide stars required for telescopes with identical aperture are not very different. Therefore, in the discussion below we rely only on Eq. (5) and assume r_0=0.20m.

Up to the present time, the most likely guide stars are generated by Rayleigh scattering in the low atmosphere and the resonant scattering of sodium D_2 rays. The typical heights are, respectively, 92 and 12km. Together with r_0, these values are substituted into Eq. (5), and then the number of guide stars for the telescope with D=2m is 1.2 and 67. For a telescope with d=4m, the respective values are 5 and 268. The corresponding results given from 1.25($\Delta\phi \leq \lambda/10$) given in [4] are, in sequence, 3, 171, 12, and 685. We can see that the number of guide stars required for partial corrections is considerably reduced. Therefore, it is easier to realize than under the conventional systems.

IV. Requirements on Guide Star Brightness in Partial-Correction Systems

In a fairly recent paper [6], the authors discussed the brightness requirements of guide stars in a circular aperture system. Here, the relationship for a square aperture system will be presented. In addition, the principal results will be listed for comparison.

The requirements on guide star brightness are also determined by the performance of the adaptive optical telescope to be

expected. In other words, the rms value $\Delta\phi$ of the residual wavefront error at the aperture plane after correction can be considered as composed of two portions: one portion is caused by the inclination of the wave plane, and the other portion is the other wavefront error outside the wave plane inclination. Indicated with the difference in optical paths with wavelength taken as unity, the latter portion error at the aperture plane d for diameter or side length is

$$\Delta\varphi_1 = (d/r_0)^{5/6} (\lambda/17.4) \tag{6}$$

The adaptive optical system corrects mainly the first portion, that is the error in wave plane inclination. After correction, the wave plane inclination error is

$$\Delta\varphi_2 = \Delta\psi d/4 \tag{7}$$

However, after correction the overall wavefront difference of the aperture is

$$\Delta\varphi = (\Delta\varphi_1^2 + \Delta\varphi_2^2)^{1/2} \tag{8}$$

In the equation, $\Delta\phi$ is the measurement accuracy of the wavefront inclination rate; this is related to the type and performance of sensing, and is determined by the density N of the signal photon current. For a Hartmann sensor, when d is greater than r_0,

$$\Delta\psi = 0.61\lambda\eta_c / (\sqrt{N} r_0) \tag{9}$$

However, when d is less than or equal to r_0, $\Delta\psi$ is also related to aperture shape. With respect to a circular aperture,

$$\Delta\psi = 0.61\lambda\eta_c / (\sqrt{N} d)$$

However, with respect to a square aperture

$$\Delta\psi = 0.52\lambda\eta_c / (\sqrt{N} d)$$

In the equations, N is the overall photon flow in the single Hartmann aperture, η_c is the factor determined by imperfections in the system. The typical value is between 1.35 and 1.50. These $\Delta\phi$ values are substituted in Eq. (7) and then we obtain

$$\Delta\varphi = \begin{cases} (0.15\lambda\eta_c/\sqrt{N})\ (d/r_0) & d>r_0 \\ 0.15\lambda\eta_c/\sqrt{N} \quad \text{圆孔}^1 & d\leqslant r_0 \\ 0.13\lambda\eta_c/\sqrt{N} \quad \text{方孔}^2 & \end{cases}$$

KEY: 1 - circular aperture 2 - square aperture

For a partial-correction system, the main interest is the situation when $d>r_0$, then

$$\text{or} \qquad \Delta\varphi = \{(d/r_0)^{5/3}\ (\lambda/17.4)^2 + (d/r_0)^2\ (0.15\lambda\eta_c/\sqrt{N})^2\}$$

$$N = (0.15^2\lambda^2\eta_c^2d^2/r_0^2)\ \{\Delta\varphi^2 - (d/r_0)^{5/3}\ (\lambda/17.4)^2\}^{-1}$$

For a circular aperture, the density of the photon current is

$$F = 8.99\eta_c^2/\{r_0^2\ [(1.74\Delta\varphi/\lambda)^2 - (d/r_0)^{5/3}]\} \tag{10}$$

However, for a square aperture,

$$F = 7.06\eta_c^2/\{r_0^2\ [(1.74\Delta\varphi/\lambda)^2 - (d/r_0)^{5/3}]\} \tag{11}$$

Again, we assume $\Delta\phi=0.13\lambda$. From reference [7], the optimal value of d/r_0 is 2. By using $r_0=0.20$m and $\eta_c=1.35$, we obtain $F=8.4/r_0^2$ (with respect to circular aperture), and $F=6.6/r_0^2$ (with respect to square aperture). However, based on the above-mentioned papers, for $\Delta\phi=\lambda/15$, the photon flow density is $38.7/r_0^2$.

V. Laser Energy

By citing the example of sodium guide stars, the total laser energy required for N_0 guide stars is [7]

$$E = (4\pi h_0^2hc/\eta T_A^2C_s\sigma_t\lambda_L)\ N_0F \tag{12}$$

In the equation, η is the efficiency (7.5%) of the telescope and detector. η_t is the sodium-resonant scattering cross-section,

$8.27 \times 10^{-16} m^2$. T_A is the single-pass atmospheric transmissibility at 0.85. C_S is the sodium-column abundance, $5 \times 10^{-13} m^{-2}$. h_g is the height (92km) of the guide stars over the telescope. $\lambda_L K$ is the laser wavelength, 589nm. h is the Planck constant, $6.63 \times 10^{-34} (J \cdot s)$. c is the speed of light, $3 \times 10^8 m/s$. The above-mentioned typical data and the derived photon current density are substituted into Eq. (12). We can obtain the following: for the laser energy required to generate a single guide star: 0.14mJ for a circular aperture, and 0.11mJ for a square aperture. From the discussion in the third section of the present article, we know that the number of guide stars required are, respectively, 1.2 and 5 required for partial correction conditions considered in the paper for telescopes with apertures 2 and 4m. Therefore, the total laser energy required to generate these guide stars is, respectively, 0.17 and 0.70mJ for a circular aperture, and 0.13 and 0.55mJ for a square aperture. For other conditions remaining the same, if $\Delta\phi = \lambda/1.75$, the diameters for a circular aperture telescope are 2 and 4m, as given in reference [7]. The laser energies required to generate guide stars are, respectively, 1.44 and 5.76mJ.

VI. Conclusions

For an adaptive-optical imaging system, for a Strehl ratio of 7.5 (the residual wavefront error is 0.13λ for the corresponding aperture, there are interdependent relationships between the number of guide stars nd the guide star brightness required, on the one hand, and the atmospheric conditions, telescope aperture, and guide

star height, on the other. Based on these relationship equations, calculations were made based on some typical data. By comparing the results obtained and the corresponding values for perfect correction in the related reference papers, the number of guide stars required is apparently reduced, and the required photon current density is rapidly reduced. In proportion to the multiplication product of the two, the laser energy for generating a guide star is further drastically reduced. These indicate that rational partial correction can dramatically simplify the system, thus further pushing the adaptive optics toward practical applications.

Resumes of the authors: Yan Jixiang, male, was born in December 1948. As an associate professor and member of the SPIE/COS, he engages at present in optoelectronic statistics, adaptive optics, as well as research and teaching on laser theory and technology. Zhou Renzhong, male, was born in 1932, as a professor and SPIE/COS member, as well as deputy director and secretary-general of the Optoelectronics Technology Committee of the China Optical Society, he engages currently in research into adaptive optics, optoelectronics design, and optoelectronic technology. Yu Xin, male, was born in 1941. As professor, OSA member, and executive deputy director of the Optoelectronics Technology Committee of the China Optical Society, he currently engages in research into adaptive optics and optoelectronic detection.

The research was funded by the State Natural Science

Foundation. The paper was received for publication on September 4, 1992.

REFERENCES

[1] Foy R, Labeyrie A. Astronomy & Astrophys, 1985; 152: 129~131
[2] Thompson L A, Gardner C S. Nature, 1987; 328: 229~231

MILITARY MID- AND LOW-POWERED CO_2 LASER TECHNOLOGY

Feng Hongyuan

Southwest Institute of Technical Physics, Chengdu 610041

Abstract: The development situation of the military laser technology is reviewed. It is proposed that the important subject in this area should be heterodyne CO_2 lidar in our country.

I. Introduction

Rapidly developed in the sixties, laser technology has extensively penetrated into science, technology, industrial and agricultural production, medical therapy, public health, and the military. In military applications of radar, there are mostly five areas, as follows: 1. ranging and target guidance (laser guidance), and laser radar. 2. Destructive directed-energy laser weapons (strategic and tactical laser weapons). 3. Laser gyroscope guidance technique. 4. Laser communications, and 5. Laser simulation training equipment. In the first item, laser ranging/target guidance (laser guidance and laser radar) has been studied for more than two decades. This area stands as the most important part of military laser weaponry.

The early sixties were not long after the appearance of lasers. At the Hughes Corporation in the United States, the first primitive ruby pulsed laser ranging device was successfully developed. Since then, laser ranging has become the most widely applied and indispensable equipment for the military. From the United States Defense Department, in military lasers the investment on mid- and low-powered laser ranging/target guidance is the most successful project for investments in the past 20 years. Due to the application of these instruments and items of equipment, the battle effectiveness of the United States Armed Forces has been upgraded by nearly one order of magnitude.

Laser ranging has completely replaced the previous conventional optical ranging. The fundamental principle is to measure the time required for the laser beam from emission to arrival at the target and be reflected. Actually, laser ranging is a laser radar with simplified functions. Since the laser beam is narrower than the conventional radar beam, as the pulse width between several to scores of nanoseconds, the distance resolving power and the ranging accuracy of the conventional laser ranging device is higher than conventional radar. Generally, the accuracy of military laser ranging devices is 2 to 5m; a precise laser ranging may reach even down to the centimeter level. Measurements path for laser ranging, owing to greater attenuation due to the atmosphere near the ground, generally has an accuracy lower than that for conventional radar. However, the measurement paths at high altitudes (or deep space) and vertical paths, the

accuracy is higher. At present, measurement paths of a military ranging device is several to tens of kilometers. The weight of a laser ranging device is also reduced from tens of kilograms at the beginning to only several hundreds of grams as the percent-day ranging telescope.

Recalling history, we see that the laser ranging device generally passed through three development stages. These are the primitive stage represented by the ruby laser ranging device, the practical stage with higher efficiency Nd:YAG as the light source and silicon snow light diode as the detecting device, and, recently developed, a laser ranging device that adopts various wavebands safe to human sight, and the introduction of heterodyne reception for carrying out the ranging, speed measurement, or even imaging in the multifunctional observation, aiming, and measurement integration system as the third stage. This actually is the development from simple laser ranging to a laser radar system with complete radar functions. This system will be the principal tool in the battlefield of the nineties.

The key to laser ranging includes the laser light source and the detection elements. Whatever the laser, the YAG laser ranging device is the most widely used, and the most mature in technique; however, since it operates in the 1.06micrometer wavelength, it is very unsafe to human sight. In addition, a laser at this wavelength is easily affected by atmospheric conditions and smoke in the battlefield, therefore its application is limited. As early as the seventies, researchers

proposed the concept of laser ranging with safety for human sight. Later on, the CO_2 laser operating at 10.6micrometer wavelength gradually appeared; the Ho:YULF laser, at 1.73micrometer wavelength; the Er:YLF laser, at 1.73micrometer wavelength; and the Nd:YAG Raman frequency-shift 1.54micrometer laser, as well as the 1.54micrometer wavelength erbium glass laser ranging device, which passed evaluation certification by the United States Army in 1985. Under present technical conditions, at the wavelengths of 2.06 and 1.73micrometers, no highly sensitive detection devices suitable for ranging have been found and therefore developments have been slow. Only the 10.6micrometer CO_2 and the 1.54 micrometer Raman frequency-shift and the erbium glass laser ranging devices are receiving most interest. These lasers have reached the level of practicality. From Table 1, the listed specification of hygienically protected standards by Stanag 3606 of the United States, the 1.54micrometer laser ranging device is the safest. The energy of a pulse of the CO_2 laser ranging device is in the range of scores of millijoules. Therefore, from the standard of Table 1, the CO_2 laser ranging device is also zero-distance safe. However, since the CO_2 laser ranging technique is complex, and almost 10,000V at high voltage (or a radio-frequency power supply is required, in addition to expensive HgCdTe, and a detection device as well as specialized infrared optical materials, apparently only from the safety significance, the performance-price ratio of the CO_2 laser ranging device is well below that of the 1.54micrometer laser

ranging device. Notwithstanding, the authors still consider that the CO_2 laser ranging technology still is highly viable. This represents the new-generation military laser system in its development direction. The light force is included in overall consideration of the development demand in the future battlefield. In addition, the CO_2 laser has many advantages that other lasers lack or are deficient in. Generally speaking, there are the following points to be considered:

TABLE 1. Human Vision Safety Standards of Stanag 3605 Laser

激光器 a	波长 b	允许最大曝光量 (J/cm²) c 重复频率(1Hz) d	重复频率(10Hz) d
红宝石 e	0.6943	5×10^{-7}	
Nd：YAG	1.06	5×10^{-6}	1.6×10^{-6}
铒玻璃 f	1.54	1	1×10^{-2}
CO_2	10.6	1×10^{-2}	3×10^{-3}

KEY: a - laser device b - wavelength c - maximum available light exposure d - repetition frequency e - ruby f - erbium glass

(1) Its operating wavelength is the same as the infrared thermal imaging instruments (FLIR) of the 8 to 12micrometer waveband as extensively applied in tomorrow's battlefield. Therefore, there are the same capabilities of transmission performance, as well as penetration through smoke, rain, fog, and frost. Therefore, both have excellent compatibility. Based on the specifications required by the United States Army on compatibility requirements on laser ranging and thermal imaging instruments, when the probability that a thermal imaging instrument can observe the target is 50%, the compatible laser

ranging device should have a probability of 99% of detecting such target in the first emission. Apparently the laser ranging device of other wavelengths is not able to meet this requirement. Besides, due to the same wavelength, the CO_2 laser ranging device can share the same optical system, detectors and refrigerator, with a thermal imaging instrument, thus constituting a compact structure and compatible performance in the integration of multiple functions in observation, aiming, and surveying in optoelectronic fire control systems.

(2) The efficiency of the CO_2 laser device (including the waveguide CO_2 laser device and the TEA CO_2 laser device) is high, generally between 8 and 10%, suitable for being built into a high-repetition-frequency CO_2 laser ranging device. Power source modulation or electrooptical modulation Q is applied for the waveguide CO_2 laser device with repetition frequency as high as tens to hundreds of kilohertz. However, for the repetition-frequency TEA CO_2 laser device, the repetition frequency may be as high as thousands of hertz; for mixed-type TEA frequency, it may attain as high as hundreds of hertz. Since the CO_2 laser device is high in frequency with convenient cooling, operating at a high repetition frequency, the dimensions and weight of a CO_2 laser system will not be greater than those of a YAG laser device with the same repetition frequency. However, in the engineering perspective, there are many practical difficulties for the YAG laser device to be operating at the repetition frequency at hundreds or even thousands of hertz, or even an impossibility.

However, in the future battlefield, for tracking high-speed, low-altitude targets, or for flight near the ground, and for an aircraft collision prevention system it is required to use a high-repetition frequency device in the laser guidance system. Therefore, the development of a high-repetition-frequency laser ranging system is a practical demand for future battlefields.

(3) The 10.6micrometer CO_2 laser has good capability in penetrating fog, frost and battlefield smoke in the atmosphere. Although the author does not have detailed data concerning the penetrating ability of the 1.54micrometer laser, yet Table 2 lists the absorption coefficients of battlefield smoke at several laser wavelengths.

TABLE 2. Absorption Coefficients (m^2/g) of Battlefield Smoke Relative to Lasers at Several Wavelengths

	可见光 e	1.06μm	3~5μm	10.6μm	8~12μm
油雾 a	3.2	3.64	0.36	0.047	0.10
红磷 b	3.36	1.93	0.29	0.47	0.27
酸雾 c	3.85	2.19	0.17	0.15	0.23
六氯乙烷 d	2.38	3.0	0.20	0.79	0.53

KEY: a - oily fog b - red phosphorus
c - acid fog d - carbon trichloride
e - visible light

As indicated from comparative results of a CO_2 ranging device, the YAG, and the 1.54micrometer ranging device, recently studied by the author, the ability to penetrate battlefield smoke by the CO_2 laser is definitely much better than for the YAG, and basically corresponds to the 1.54micrometer laser, or even

better. The data are also basically matched with the experimental data [4] from abroad concerning the penetrating ability through battlefield smoke by the 10.6micrometer laser.

(4) A set of CO_2 laser devices can very conveniently execute an output of multiple spectral lines for selective modulation. If consideration is given to the transition of the sequential band of an isotopic CO_2 laser device and a CO_2 laser, the selective wavelength range for a CO_2 laser is quite wide. By using these selective modulation properties for optical heterodyne communications, or atmospheric remote sensing and battlefield toxicity measurement, there are very good application prospects for the battlefield of the future in the nineties.

(5) The wavelengths of the CO_2 laser is relatively long. Since the coherence with the long wavelength atmospheric turbulence flow is much weaker than those of short wavelengths, such as in the situation of intensive eddy currents ($C_N=10^{-13}m3/2$), the coherence reception radius of 1.6micrometers at a horizontal transmission distance of 10km is only 1/25 of that for a 10.6micrometer wavelength; this comes out, approximately, to 0.4cm. Therefore, in applications of the near-ground surface for horizontal distance, the long wavelength is very beneficial for heterodyne reception. Based on theoretical calculations, if it is assumed that all reception is restricted by noise of scattered particles, then the detection sensitivity of heterodyne reception is higher, by eight orders of magnitude in sensitivity, than for direct detection. The sensitivity of an

actual system is also different, by 10^3 to 10^4. Therefore, for heterodyne detection of the same measurement range, the emission power can be greatly reduced. In addition, it is possible to conduct rapid selective wide-range modulation, the confidentiality and freedom from jamming are very high. Besides, the system can also do range and speed measurements. The ranging accuracy is in the meter level, and the accuracy of speed measurements is also better than 1m/s. These properties are not able to be attained by a direct detection approach.

Based on the above-mentioned advantages, the authors consider that, militarily, in the future the CO_2 laser technology has great potential. Of course, some technical difficulties still exist at present. However, with the development of technology of the components, the size, weight, reliability, and cost of the CO_2 laser system will be gradually improved. For example, the dimensions of a small high-voltage power source can be reduced by 70%, although in operating performance of cost the HgCdTe detector has some difficulties, yet as stated by some people in this field, the detection components of the CO_2 laser at present resemble the silicon detection components of 1.06micrometers more than 10 years ago, technology will gradually mature with developments, thus the various present-day problems will be solved.

II. General Development Situation of Military CO_2 Laser Systems

The development of military CO_2 laser systems is torturous

and lengthy. In the past period of more than two decades there were several ups and downs. As early as the late sixties, M. G. Teich perfected the technical theory of heterodyne reception with CO_2 [2]; at that time, the heterodyne laser radar and optical communication system (for atmosphere and deep space) were met with researchers' enthusiasm. However, due to a lack of maturity of the components, the reliability, service life, modulation, and reception of the basic components of the CO_2 did not pass the acceptance level. Therefore, only some fundamental experimental research could be conducted on the heterodyne CO_2 laser technology without any practical progress. Later on, in the early seventies, due to the emergence of the TEA CO_2 laser device [3,4] and the waveguide CO_2 laser device [5], with subsequent solutions of service life, reliability, frequency stability, and modulation techniques of the sealing-off devices, in addition to the scanning technique as well as other technical problems, such as refrigeration of the wideband HgCdTe detectors, this laid a solid foundation for the development of the second stage in military CO_2 laser technology. In 1974, the experimental results [6] of the continuous wave modulation frequency (FM-CW) heterodyne CO_2 laser radar were reported. Not long afterwards, in 1978, the RSRE reported a pulsed CO_2 laser ranging device [7] with direct detection. Thereafter, there was a developmental high tide in military CO_2 laser technology. Whether in direct detection or in heterodyne detection, all the military CO_2 laser systems have seen practical progress. Table 3 listed the

progress with military CO_2 laser technology.

There are the following representative products in the military CO_2 laser systems: from the Feilandi Corporation in the United Kingdom, there are models 303, 307, 311 direct-detection CO_2 laser ranging devices, and heterodyne receiving model 305 CO_2 laser ranging devices [8], the model 116 high-repetition direct-detection CO_2 laser ranging device [9]; from RSRE, there are heterodyne CO_2 laser ranging instruments [10]; from the GTE Sylvania Corporation in the United States, there is the precise tracking system (PATS) [11]; from the Lincoln Laboratories, there

TABLE 3. Technical Progress in Military CO_2 Lasers

Year	Status of Progress
1964	Realization of CO_2 light oscillations
1966	Realization of heterodyne reception of 10.6micrometer CO_2 laser
1968-1971	Realization of heterodyne mixing of HgCdTe device with comprehensive theoretical research on CO_2 heterodyne reception technology
1970-1972	Development of waveguide CO_2 laser device and TEA CO_2 laser device
1970-1976	Successful development of continuous-wave modulation frequency of heterodyne CO_2 laser radar and pulsed CO_2 radar; and attainment of waveguide CO_2 laser system for satellite communications

Year	Status of Progress
1975-1978	Practical applications of DC waveguide CO_2 laser device and realization of radio-frequency-excited waveguide CO_2 laser device; and attainment of TEA CO_2 laser device with long-lived sealing-off model Development of first set of direct-detection pulsed CO_2 laser ranging device. Successful development of CO_2 laser target indicator; development of research in engineering CO_2 laser radar, thus the military laser technology enters the engineering development stage from the laboratory.
1980	In several western countries, successful developments of prototypes of various CO_2 laser devices with evaluation testing.
1981	Realization of three-frequency heterodyne reception and carrying out of full-wave mixed-frequency experiments on theoretical principles.
1985	Accomplishment of engineering development of TEA CO_2 laser ranging device.
1987	Accomplishment of forerunning work before beginning of batch production of TEA CO_2 laser ranging device
after 1990	Assembly of CO_2 laser ranging devices.

is the Fire Pond system [12]; from the DREV Corporation in the United Kingdom, there is the mixed model TEA CO_2 laser ranging device [13]; from the TPC in France, there are the model 137 direct-detection pulsed CO_2 laser ranging device and the THC model 198 heterodyne pulsed CO_2 laser ranging device; and from Texas Instruments Corporation in the United States, there is the laser/thermal imaging instrument combination ranging device [14], among others. In these CO_2 laser systems, the laser devices adopted include the TEA CO_2 laser device, the mixed model TEA CO_2 laser device, and the waveguide CO_2 laser device. The detection methods include direct detection and heterodyne detection. The

operating frequencies of the laser device range from 1Hz to 100Hz, or even higher. We can see that the low-repetition-frequency laser ranging device and the high-repetition-frequency laser ranging device currently adopting the TEA CO_2 laser device have all completed their engineering development. The MI-A2 tanks in the United States will be deployed [15] in the early nineties. The future development direction is the development of the CO_2 laser ranging systems compatible with infrared thermal imaging instruments. Other than the CO_2 laser ranging with direct detection and with heterodyne detection, other important aspects of the military CO_2 laser are guidance, remote sensing of battlefield chemicals (toxicity detection) and CO_2 laser radar. It was reported that there are more than 10 companies in the United States, the United Kingdom, France, West Germany, and other countries, engaging in CO_2 laser heterodyne detection laser radars. From the level of practical developments, currently on the components and parts of CO_2 laser heterodyne reception technique, the development of small engineering models and modularization of CO_2 heterodyne laser devices, there are basically matured conditions. In the nineties, possibly there will be great progress. Therefore, it can be said that the present-day military CO_2 lasers have been gradually matured entering the stage of practical applications.

III. Several Views on Developing Military CO_2 Laser Systems in China

At present, development has certain foundations for military

CO_2 laser technology in China. Among them, the following devices have been successfully developed and have passed certification: small TEA CO_2 device, direct-current and radiofrequency-excited waveguide CO_2 laser device, high-repetition-frequency TEA CO_2 laser device, mixed-model TEA CO_2 laser device, and grating-modulated small waveguide CO_2 laser device. The Guangfu model HgCdTe detectors have been used in the CO_2 laser ranging devices made in China. The frequency stability of the passive stable frequency CO_2 laser device has attained an order of magnitude 10^{-6} to 10^{-7}. The techniques of NH_2D Stark Pond and the SF_6 saturation absorption pond, used for active stabilization of frequencies, were also reported. An isotopic CO_2 laser device was also successfully developed. However, there are no practical products on cryogenic techniques for detectors and techniques of active frequency-stabilized CO_2 laser device and wideband HgCdTe detectors, for heterodyne use.

As to applications of CO_2 lasers, the multichannel carrier wave of a CO_2 laser was successfully developed. Technical certification of the prototype of a portable pulsed CO_2 laser ranging device has passed; multiple field experiments were conducted. Heterodyne experiments were also conducted on the modulation waveguide CO_2 laser device.

Generally speaking, the military CO_2 laser technique in China has attained or approached the level of the early and mid-eighties abroad in research on direct-detection pulsed CO_2 laser ranging devices. However, this was just the beginning into

research on heterodyne reception technique with CO_2 lasers; this is in the early stage. To promote the development of technology in military CO_2 lasers in China, the authors have the following views:

(1) On the present research foundation of the prototype machine of the direct-detection CO_2 laser ranging device, engineering and practicality stage should be moved forward as rapidly as possible, to complete the engineering development within the Eighth Five-Year Plan Period. Moreover, resources should be allocated as early as possible to develop the high-repetition-frequency CO_2 laser ranging device. In research on the high-repetition-frequency CO_2 laser ranging device, the achievements of the low-repetition-frequency CO_2 laser ranging device should be utilized as much as possible. The maximum ranging should be determined as between 5 and 10km, and the repetition frequency should be selected between 30 and 50Hz.

(2) The development of the CO_2 laser ranging device/thermal imaging hybrid compatible system should be developed as fast as possible. The key to development lies in long service life, small high-repetition-frequency devices (ircluding catalysts), the shared substrate between the CO_2 laser and the thermal imaging instrument detector (development of a fast high-response optical guidance type HgCdTe detector), as well as research on synchronizing scan techniques.

(3) The maximum advantage of the CO_2 laser is heterodyne reception. Therefore, the research on the CW heterodyne of the

radiofrequency waveguide, and pulsed heterodyne of the mixed-type TEA CO_2 laser device should move forward in synchronous steps in order to meet the demands of different application occasions later on. Therefore, we should stress the development of frequency-stabilized radiofrequency-excited waveguide CO_2 laser devices and mixed-type TEA CO_2 laser devices, along with their modulation technique, frequency-stabilization techniques, as well as high-frequency HgCdTe devices of hundreds of megahertz in bandwidth. We should redouble our efforts to have important breakthroughs in the heterodyne reception techniques in the period of the Eighth Five-Year Plan, to develop the prototype machines of heterodyne ranging and speed measurement in order to lay a technical foundation for the development of entire machines of CO_2 laser radar in the period of the Ninth Five-Year Plan.

(4) The development of the related techniques in military CO_2 laser systems should receive attention, for example, cybernetic technique, CO_2 catalyst and regenerative technique, as well as high-repetition-frequency and long-lived fast switching techniques, optical beam modulation and demodulation techniques, as well as optical beam scanning techniques, among others.

For a brief resume of the author, Feng Hongyuan, male, was born in September 1938. As a senior engineer, he currently specializes in laser technology. The paper was received for publication on July 20, 1992.

REFERENCES

[1] Thomas C R, Chynoweth P J. CO_2 TEA laser for military applications. GEC Avionics Ltd, 1984

[2] Teich M C. Proc IEEE, 1968; 56: 671

[3] Dumanchin R, Roeca-Serra J. C R Acad Sci, 1969; 269B: 916

[4] Benulieu A J. A P L, 1970; 16: 504

[5] Bridges T J, Burkhardt E G, Smith P W. A P L, 1972; 20: 403

[6] Braunfelder M F. AD/A-005865, dec, 1974

[7] Taylor M J, Davies P H, Brown D W *et al*. Appl Opt, 1978; 17(6): 885

[8] Woods W F, Malcolm D A. Military electronics device expo' 80. Conference Proceeding, 1980

[9] Woods W F. SPIE, 1986; 806: 122

[10] Halme K F. Opt & Quant Electron, 1981; 13(1): 55

[11] SPIE Proc, 1978; 134

[12] Sullivan L I. SPIE Proc, 1978; 277: 148

[13] Craickshank J M. Appl Opt, 1979; 18: 290

[14] Patrickxhank T R. Appl Opt, 1979; 18: 290

[15] Patrick L R. USP 4,561,775, 1985

COATING OF RESONATOR MIRRORS FOR NEAR-INFRARED Na_2 OSCILLATION

Liu Jincheng, Wang Qi, Ma Zuguang

Institute of Optoelectronics, Harbin Industrial University, Harbin 150006

Abstract: In this paper, the designing and coating of special film system for near-infrared laser oscillation of Na_2 are reported. In 1988, with this film, laser oscillation of the lowest triplet transition of Na_2 was obtained for the first time.

I. INTRODUCTION

The investigation of Na_2 near-infrared oscillation is a leading topic of the early eighties, generally emphasized by the international research community in this field. In particular, the first triplet laser oscillation was predicted by Konowalow [1] in 1980 as a resonant coherent light source in the infrared range. The resonant range is between 830 and 900nm; the excited emission cross-section is 10 square angstroms. This is a new infrared resonant coherent light source with good prospects of applications in laser spectrum technology.

The first triplet transition ($b^3\Sigma_g^+ - X^3\Sigma_u^+$) laser-induced

fluorescent spectrum of Na_2 was observed in 1981 [2] (see Fig. 1). The search for laser oscillation in this spectral region has always been the aim of many countries and many research teams.

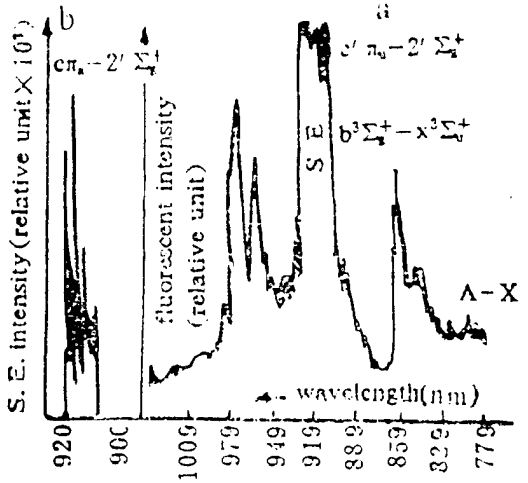

Fig. 1 Near-infrared fluorescent radiation
a—lowest-triplet transition region (830~900 nm)
b—910 nm ASE region

II. Design Considerations

From the fluorescent spectral region excitation regime for carrying the Na_2 $b^3\Sigma_g^+ - x^3\Sigma_u^+$, there are the following unique requirements on the resonator.

1. The first triplet spectral region is located in the region of 830 to 900nm. There are different peak values for the excitation regime in different regions. Based on the regime in [2], the peak is at 855.5nm. According to the regime in [3], the peak is 892nm. However, whatever the regime, there is a spontaneous radiation amplification at 911nm. The spontaneous radiation

amplification has two possible functions in laser oscillation:

(1) This is possibly the indirect pumping light exciting the Na_2 $b^3\Sigma_g^+ - x^1\Sigma_u^+$ transition, thus promoting the formation of the first triplet laser oscillation.

(2) This is possibly the radiation transition of another channel, for obtaining the upper energy level particles in competition with the first triplet state. In laser oscillation at this time, its ratio value will have a wearing down function on the first triplet laser oscillation to be obtained. Thus, its high reflection should be avoided, if possible. This is the viewpoint of this present research.

2. The more effective route in carrying out the Na_2 transition* is ultraviolet excitation. Therefore, the resonator mirror should operate under excitation of intensive ultraviolet rays. The wavelength of the pumping light is 351nm. * $b^3\Sigma_g^+ - x^3\Sigma_u^+$

In research on the Na_2 $b^3\Sigma_g^+ - x^3\Sigma_u^+$ laser oscillation, the appropriate film system of the resonant mirror should be used, with correct selection of film material. Research on coating technique and process of the resonator mirror will provide convenient conditions for generating laser oscillation. It can be stated that it is indispensable to have a resonator mirror satisfying the requirements in order to let the Na_2 $b^3\Sigma_g^+ - x^3\Sigma_u^+$ laser oscillation become a fact.

There are the following design requirements on the resonator mirror: (1) there should be high reflection at 855nm, and high

transparency at 911nm. The width (of the reflective band) $\Delta\lambda$<100nm (the center wavelength λ_0=855.5nm, plus or minus 50nm). (2) There should be high transparency at 351nm of the pumping light. (3) There should be anti-ultraviolet.

(4) There is a passband in two regions of 132.5 to 550nm, and 600 to 800nm (within the passband, there should be an absence of a reflective peak in order to avoid the gain of the Na_2 b-x band and the B-X band) in both spectral regions. (5) There should be hard film. Generally, the all-medium reflective mirror is made of high and low reflective materials, with optical thickness of $\lambda_0/4$ in the multilayer film. Theoretically, with an increase in reflectivity of the reflective mirror for the coating layer, there can be an unlimited approach to 100%. Actually, because of restrictions on film layer thickness control accuracy and absorption and scattering losses in the film layer, when the film system has a certain number of layers, that is, the reflectivity approaches 100%, the continuous coating is unable to increase the reflectivity. Conversely, owing to increased losses in absorption and scattering, the reflectivity is decreased.

In the authors' design, well-known zirconium oxide and silica are used as the cyclic alternating high- and low-reflective coating layer materials. Table 1 shows their properties.

From Table 1 [4], we can see that the transparent region meets the requirements, especially the 351nm pumping light. The same evaporative method adopted also creates convenient technical

Table 1 ZrO_2 SiO_2 properties

material	refractivity	transmissive region(μm)	evaporation art	melting point(℃)
ZrO_2	2.1 (0.55μ) 2.0 (2μ) 1.92 (1μ)	0.3~7	electron beam	2700
SiO_2	1.46 (0.55μ)	0.2~8	electron beam	1710

conditions for coating. The zirconium oxide film is hard, not absorbing humidity, with some compressive stress. The silica film is stable, firm, chemically corrosion-resistant, and has tensile stress. The high melting points of these two materials determine that films from both materials satisfy the hard-film conditions, and the stress combination is also appropriate.

For single-layer ZrO_2 and SiO_2, when the coating layer thicknesses are one-quarter of the center wavelength, the laser-damaged threshold values are 70 and 130J/mm^2, respectively. However, for 23-layer film composed of these two materials, the film system is $[HL]^{11}H$, and the laser-damaged threshold undertaken is 15J/mm^2 [4].

For alternating evaporated coating high-reflection films with thickness at one-quarter of the center wavelength, once the material is selected, correspondingly the width of the main reflection band is also determined. Let us assume that on a glass substrate with n_0=1.52, alternating evaporated and coated zirconium oxide with n_H=1.9 and silica with n_L=1.46, then the

relative width of the wave number expressing the known reflectivity to be obtained is

$$\Delta g = \frac{2}{\pi}\sin^{-1}\left(\frac{n_H - n_L}{n_H + n_L}\right) = 0.084$$

The width of the wavelength of the reflective band corresponding to the center wavelength 855.5nm is

$$\Delta\lambda \doteq 2\Delta g\lambda_0 \doteq 144 \text{ (nm)}$$

The reflectivity formula of the termination region is

$$R = \left[\frac{1 - (n_H/n_L)^{2s}(n_H^2/n_g)}{1 + (n_H/n_L)^{2s}(n_H^2/n_g)}\right]^2$$

We can easily calculate that the reflectivity can be as high as 98% when there are 17 coated layers. In the equations, s is the number of fundamental cycles.

We can see that the difficulty of satisfying the design requirements are the width of the reflective band and the region of visible light, as well as the high transparency at 351nm of the pumping light. Multiple spectral regions can simultaneously require that there is high transparency in some spectral regions, and from ultraviolet to near-infrared for high reflection in some spectral regions. This imposes certain difficulties for the $\lambda/4$ film system (refer to Fig. 2 [5]).

The width of the reflective band is determined only by the ratio value between the high and low refractivities of the film layer, therefore the width is not related to the number of layers [5]. Besides the emergence of the main reflective band at the

center wavelength λ_0, there are also high-order reflective bands (see Fig. 2) at the wavelengths $\lambda_0/3$, $\lambda_0/5$, $\lambda_0/7$, ... The widths of the relative wave number of the various reflective bands are the same, however, the corresponding widths of the wavelength are reduced in approximate ratios of 1/9, 1/25, and 1/49. Therefore, after the film material is selected, we can consider the application of high-order for the required high-reflection film of narrow band in order to meet the requirements. This is one of the principal measures in narrow-band techniques.

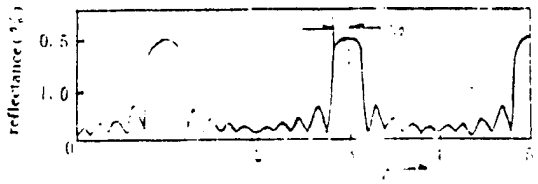

Fig. 2 Reflectivity curves of 9-layer ZeS film coated on glass ($n_2=1.52$) and icestone

If 855.5nm is the center wavelength λ_0 and we let it be at the position of the third order, we thus achieve the width of the reflective band at the compressed 855.5nm. This corresponds to a new center wavelength $\lambda_0'=3\times855.5$nm. Thus, at the wavelengths of 855.5nm ($\lambda_0'/3$), 513.3nm ($\lambda_0'/5$), and 366.6nm ($\lambda_0'/7$), the high-order reflective bands emerge. Their corresponding wavelength width are, respectively,

at 855.5nm $[\Delta\lambda]_3=\lambda_0'/(3-\Delta g)-\lambda_0'/(3+\Delta g)\doteq47.9$ (nm)

at 513.3nm $[\Delta\lambda]_5=\lambda_0'/(5-\Delta g)-\lambda_0'/(5+\Delta g)\doteq17.3$ (nm)

at 366.6nm $[\Delta\lambda]_7=\lambda_0'/(7-\Delta g)-\lambda_0'/(7+\Delta g)\doteq8.8$ (nm)

These are, respectively, approximately 1/9, 1/25, 1/49, ... of the wavelength width of the main reflective band.

Besides, to a certain wavelength λ_0, for all thicknesses as $\lambda_0/4$, for high-reflective film, and for other high-reflective films with all thicknesses as $3\lambda_0/4$, with the same ratio of values of refractivity, at the wavelength λ_0, the wavelength width of the latter high-reflection region is approximately one-third of the former.

With the above-mentioned analysis, we can see that the indicators of bandwidth can satisfy the design requirements.

If the application of the narrow-band technique shifts toward the long-wave direction for the odd-numbered multiples of the controlled wavelength, thus creating a result that although the number of film layers is not increased, yet the thickness of each film layer is considerably increased. To remedy this shortcoming, the authors let the reflective band fall onto the third-order position. Or, the film layer thickness can be considered to only increase a kind of filming material, and the thickness of the film layer of another film material is still $\lambda_0/4$. In other words, this is the use of the method of adjusting the resonant ratio to reduce the increase in film layer thickness. Thus, the cyclic film system is changed from [3H3L] to [H3L] or [3HL]. In this way, the results correspond to reducing the thickness by one-third. However, the calculation of the various orders of bandwidth for adjusting the resonant ratio of the film system, and the utilization of high-order compressive

bandwidth are basically the same.

It is relatively ideal in applying the design of other than $\lambda_0/4$ film systems; however, we still have to use the narrow-band technique to satisfy the width requirements for the reflective band. Moreover, by using the broadening technique of the passband, the restraining of the high-order reflective peaks is not required.

The coating layer monitoring method for thickness other than $\lambda_0/4$ wavelength is the so-called quartz crystal oscillation method.

Due to restrictions on equipment conditions, only the curve for the theoretical transmission rate is given for the film system and computer-based calculation (Fig. 3, not included).

The film system adopted is

Among these,

$$n_A = 1.46 \quad n_B = 1.9 \quad n_C = 2.39$$

$$G: n_J = 1.49 \qquad M: n_M = 1.0$$

thickness $\quad A \cdot B = \frac{\lambda_0'}{24} \qquad C = \frac{\lambda_0'}{3} \qquad s = 7$

From Fig. 3, we can see that this is an ideal film system. Although the number of film thickness is comparatively more, yet the thickness of each layer is much thinner. Further investigation can be conducted when there are appropriate conditions.

III. Coating and Preparation of Films

1. Installation

(1) In experiments, the film-coating machine is a DMD-450 model optical multilayer film-coating machine, made by the Beijing Instrument Plant. After remodeling, a magnetic deflected type e electron gun was installed. The maximum upper power is 3kW. The high voltage output is between 0 and 10kW, adjustable. The output beam current is 0 to 300mA, adjustable.

(2) The model number of the detector is 9684B (made in the United Kingdom) optoelectronic gain tube, with a sensitivity region between 700 and 900nm.

(3) The monitoring instrument is a model MKY optical film thickness control instrument, made by the Shenyang Institute of Instruments and Meters.

Table 2 Evaporation art parameters

material	heater current(A)	negative voltage(kV)	beam current(mA)	power (W)	focal spot area(mm^2)	power density (W/mm^2)	evaporating time (min)
ZrO_2	14	9	90	810	113	7.2	$\lambda_0/4$ thk 1.2
SiO_2	11	11	60	660	113	5.8	$3\lambda_0/4$ thk 1.2

2. Meters

The evaporation coating materials are zirconium oxide and silica; they are white substances in small cylinders made by the Beijing General Academy of Nonferrous Metals. Their purity is 99.9%.

Refer to Table 2 for evaporation art parameters.

3. Film system, technical process and explanations

(1) The film system is designed as $G|(H3L)^7H|A$. Refer to Fig. 4 (not included) for its theoretical calculation curve.

(2) 3L has a thickness of $\lambda_0'/4$. If the center wavelength is controlled at 855.5nm, then there will be three polar value points, indicating the increasing control accuracy.

(3) Zirconium oxide is a high-melting-point material. During evaporative coating, we should note that the power density should not be too high in order to have chemical breakdown due to overheating. If there are appropriate technical conditions, evaporation with the filling of oxygen can be conducted.

(4) The temperature of the base plate is approximately 250°C. Thus, the filming effect of ZrO_2 and SrO_2 will be better.

(5) After the finished product is taken out of the vacuum chamber, the product should be placed into a baking oven to be heated over 250°C for time-effect treatment. Generally, the time required is more than 4h.

(6) When coating, a quartz wafer (n_9=1.46) is used as the base for coating of 21 layers. The number of coating layers is slightly more than the theoretical calculation. This is the result of desired reflectivity.

(7) From Fig. 5, we can see that the first wave fluctuation in the right-hand part of the passband of the reflective band is slightly lower; this is due to polar value control. It is required to ensure that the value accuracy of each layer to be accurate, thus the effect will be good.

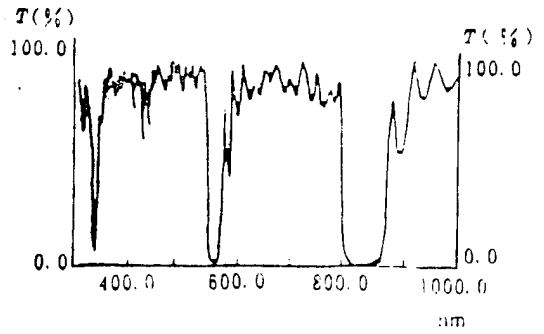

Fig. 5 Practical transmissivity curves of coated elements

V. Results

Testing of the measured curve was conducted on a Hitachi U-3400 spectrophotometer. From comparison between measured curve and theoretical calculations (Fig. 5 and Fig. 4 (not included)), we can see that the coating is successful, satisfying the design requirements of various spectral regions:

T=70% for 351nm; T=82% for 911nm

Both spectral regions of 432.5 to 550nm, and 600 to 800nm are passbands.

The location of 855.5nm is within the high-reflective band with R>99% and $\Delta\lambda$<100nm.

As mentioned above, by using the resonator coated and prepared by the authors, in 1988, the Na_2 first triplet laser resonance [3] was carried out for the first time, internationally.

Resume of one of the authors: Liu Jincheng, male, was born in 1945. As an engineer, he is currently engaged in research on

high-power laser technology, mainly on thin-film techniques.

The paper was received for publication on September 14, 1992.

REFERENCES

[1] Konowalow D D, Rosenkromtz M E, Olson M L. J Chem Phys, 1980; 72(4): 2613

[2] 马祖光. 光学学报, 1982; 2(3): 233

[3] Wang Qi, Lu Zhiwei, Liu Wei *et al*. $Na_2 1^3\Sigma_g^+ - 1^3\Sigma_u^+$ lasing with peak around 892.0nm. AIP Conf Proc, 1989; 191: 578

[4] 光学薄膜编写组. 光学薄膜. 上海: 人民出版社, 1976: 43～44, 104～105

[5] 唐晋发, 顾培夫. 薄膜光学与技术. 北京: 机械工业出版社, 1989: 77,179

DISTRIBUTION LIST

DISTRIBUTION DIRECT TO RECIPIENT

ORGANIZATION	MICROFICHE
B085 DIA/RTS-2FI	1
C509 BALL0C509 BALLISTIC RES LAB	1
C510 R&T LABS/AVEADCOM	1
C513 ARRADCOM	1
C535 AVRADCOM/TSARCOM	1
C539 TRASANA	1
Q592 FSTC	4
Q619 MSIC REDSTONE	1
Q008 NTIC	1
Q043 AFMIC-IS	1
E404 AEDC/DOF	1
E410 AFDTC/IN	1
E429 SD/IND	1
P005 DOE/ISA/DDI	1
1051 AFIT/LDE	1
P090 NSA/CDB	1

Microfiche Nbr: FTD95C000756
NAIC-ID(RS)T-0495-95